Геология и геофизика, 2021, т. 62, № 7, с. 976— 987

УДК 552.3+552.5(510)

ИССЛЕДОВАНИЕ ГЕОСТАТИСТИЧЕСКОЙ ИНВЕРСИИ В ЛИТОЛОГИЧЕСКОМ РАСПРЕДЕЛЕНИИ И СКОРОСТНОМ МОДЕЛИРОВАНИИ МАГМАТИЧЕСКИХ ТЕЛ БОЛЬШОЙ МОЩНОСТИ В ОБЛАСТИ ФУЮАНЬ СЕВЕРНОЙ ЧАСТИ ТАРИМСКОГО БАССЕЙНА (*Китай*)

Ю. Сюй[1], Х. Ян[2], Г. Пэн[2], С. Дэн[2], Ц. Мяо[2], И. Ма[1], Ц. Лю[1,3]

[1]*School of Resources and Geosciences, China University of Mining and Technology, Xuzhou, 221116, China*

[2]*Institute of China Petroleum Tarim Oilfield Company, Korla, 841000, China*

[3]*School of Nuclear Science and Technology, Lanzhou University, Lanzhou, 730000, China*

В северной части Таримского бассейна при бурении пермских отложений выявлено большое количество мощных магматических тел. Их литология и скорости сейсмических волн в них резко изменяются, что оказывает значительное влияние на миграционное изображение «бусиновидных» отражений. Для разведки и разработки коллекторов очень важно проводить детальное литологическое определение и высокоточное скоростное моделирование магматических пород. В настоящей статье приводится метод геостатистической инверсии для определения закономерностей литологического распределения магматических пород и скоростного моделирования в области Фуюань северной части Таримского бассейна. Результаты показывают, что применение метода геостатистической инверсии значительно повышает разрешение литологических определений, что помогает лучше понять распределение пермских магматических пород в области Фуюань. Сравнение классификационных карт сейсмических фаций области исследования показывает, что полученная скоростная модель хорошо отражает латеральное распределение магматических пород. Также данная модель подробно и с большой точностью определяет изменения скоростей в магматических породах. Средняя ошибка определения скорости в скважинах, используемых в инверсии, составляет менее 2 %, а минимальная средняя ошибка скорости — 0.23 %. Полученная скоростная модель была использована для обработки сейсмических данных. Результаты обработки показывают, что данная модель позволяет улучшить сейсмическое миграционное изображение. Проведённые исследования демонстрируют, что метод геостатистической инверсии позволяет получить высокоточную скоростную модель для прогноза пластового давления и обработки и интерпретации данных сейсмики, а также задавать направление разведке и разработке нефти.

Магматические породы большой мощности, геостатистическая инверсия, литологическое распределение, скоростное моделирование

STUDY OF GEOSTATISTICAL INVERSION IN THE LITHOLOGIC DISTRIBUTION AND VELOCITY MODELING OF THICK IGNEOUS ROCK IN THE FY AREA, NORTHERN TARIM BASIN, CHINA

Y. Xu, H. Yang, G. Peng, X. Deng, Q. Miao, Y. Ma, J. Liu

In the northern Tarim Basin, a large number of thick igneous rocks are encountered in the drilling process in the Permian. Their lithology and velocity are very strongly, which has a great influence on migration imaging of the “beaded” areas. It is very important to conduct the fine lithology identification and high-precision velocity modeling of the igneous rocks for the exploration and development of the reservoirs. A geostatistical inversion method to obtain the igneous-rock lithologic distribution pattern and velocity modeling in the FY area of the northern Tarim Basin is introduced in this paper. The results show that the application of the geostatistical inversion method greatly improves the resolution of lithology identification. This helps us further understand the Permian igneous rocks distribution in the FY area. Comparison between the seismic facies classification maps of the FY study area shows that the obtained velocity model can reflect the lateral distribution of igneous rocks well. At the same time, the velocity model can reflect the variation of igneous rocks velocity in detail and has a high precision. The average velocity error of the wells participating in the inversion is less than 2%, and the minimum average velocity error is 0.23%. Finally, the velocity model is applied to seismic data processing, and the processing results indicate that it can help to improve seismic migration imaging. The study demonstrates that the geostatistical inversion method can provide a high-precision velocity model for formation pressure prediction and seismic data processing and interpretation, ultimately guiding the exploration and development of oil.

Thick igneous rocks; geostatistical inversion; lithology distribution; velocity modeling

---

✉e-mail: liujt@cumt.edu.cn

DOI: 10.15372/GiG2019168

INTRODUCTION

In the northern Tarim Basin, there are widely distributed igneous rocks. The lithology of igneous rocks changes abruptly in both the vertical and horizontal directions. The velocity of different igneous rocks varies greatly, and the high-precision velocity model is one of the cores of prestack depth migration. The unclear understanding of igneous lithology and velocity has a great influence on the exploration and development of oil. A lot of works have been carried out to solve the difficult problems of rock lithology identification and velocity modeling. The BP neural network is utilized to identify igneous rock with poor reflection energy and poor continuity, which can provide a more reliable basis for the deployment of new wells (Zhang et al., 2003). Seismic attributes, rock physical characteristics, seismic inversion, and seismic forward modeling are combined with the characteristics of igneous rock in the Tazhong area, and a better understanding of the igneous rock in the study area is obtained (Luo, 2006). To obtain the velocity characteristics of igneous rocks accurately, probabilistic neural network inversion and seismic multiattribute analysis are used to establish the velocity field of Tabei in Xinjiang, which is in conformity with the geologic characteristics (Xie et al., 2015). A contrastive study of the method determining the lithology and velocity of Permian igneous rocks, such as constrained sparse-spike inversion, artificial neural network inversion, and logging multiparameter inversion, is carried out. The results show that the fast modeling based on constrained sparse-pulse inversion is more suitable for velocity modeling (Cui et al., 2016). Ambient noise tomography is utilized to study the velocity structure of the basalt and subbasalt, and a more structurally complex and laterally heterogeneous crust is obtained (Sammarco et al., 2017). Seismic interpretation, artificial neural networks, and model-based inversion are adopted to study the seismic response of the igneous intrusions and lava flows (Naviset et al., 2017).

In the above works, conventional methods of wave impedance inversion and velocity modeling are used to study igneous rock. The common problem is that the vertical resolution is not enough to distinguish the thin interbed, which will result in inaccurate lithology and velocity prediction. The complex lithology of igneous rock with great thickness and velocity variation in the FY area can be broadly divided into three types: dacite, basalt, and pyroclastic rocks. The seismic reflection characteristics of the dacite are as follows: The reflection energy is weak; the continuity of the seismic event is poor; and the amplitude varies greatly. Basalt has stronger reflection energy but a small thickness. The pyroclastic rocks are thick, and their lithology is complex. All those characteristics make it difficult to use conventional seismic inversion methods to finely identify the complex lithology of the igneous rock in the FY area. Geostatistical inversion combines deterministic inversion with stochastic simulation can finely depict the thin interbed and improve the resolution of the lithologic inversion result (Yu and He, 2013; Shen et al., 2016; Zhang et al., 2016). A method based on geostatistical inversion of igneous rock is introduced to understand the lithology and velocity distribution pattern of the thick igneous rocks in the FY area more accurately and to obtain the high-precision velocity data on the Permian igneous rocks with a view to guiding the work of oil exploration and development.

METHODOLOGY

Geostatistical inversion method

The geostatistical inversion method combines the stochastic simulation with the seismic inversion, which is actually a process of optimizing the multiple simulation results on the basis of stochastic simulation and the understanding of geological data in the work area (Wang and Wang, 2013; Tamaki et al., 2016; Bellatreche et al., 2017; Pereira et al., 2017; Sabeti et al., 2017). The Bayes discriminant theory and the Markov chain Monte Carlo sampling algorithm are the two cores of geostatistical inversion. The Bayes discriminant theory can combine with seismic, logging, and geological prior information, so that the posterior probability density function of a lithologic body is obtained. The Bayes formula is expressed as:

$$p(X \mid H, E) = \frac{p(X \mid H) p(E \mid X)}{P(E \mid X)}, \tag{1}$$

where $p(X|H, E)$ is the posterior probability density function; $p(X|H)$ is the prior distribution of parameter X under the condition of hypothesis H; $p(E|X)$ is a likelihood function observed under known X conditions; $P(E|H)$ is the regular factor.

However, one lithology or lithofacies often corresponds to multiple attribute parameters. In practice, it is difficult to solve the posterior probability density distribution function, while the Markov chain Monte Carlo sampling algorithm provides a solution. The basic idea of the algorithm can be summarized as follows:

(1) Constructing a Markov chain and converging it to a stationary distribution $\pi(x)$;

(2) Generating a sample: Starting from point $x^{(0)}$ in a certain space Φ, n is the total number of generated samples, sampling with the Markov chain in (1) and generating a point sequence: $x^{(1)}$, $x^{(2)}$, ..., $x^{(n)}$;

(3) Monte Carlo integration. m is the number of samples when the chain is smooth; the expection estimation of any function $f(x)$ is

$$\mathrm{E}[f(x)] = \frac{1}{n-m}\sum_{t=m+1}^{n} f(x^{(t)})\,. \tag{2}$$

Establishment of lithology curve

Sensitive parameter analysis of different lithologies of igneous rocks is a prerequisite for geostatistical inversion. Through sensitivity analysis, the parameters which are sensitive to lithology of igneous rocks are found, such as wave impedance, natural gamma, etc. They are used for classification of lithology, analysis of geostatistical parameters, and subsequent geostatistical inversion. With regard to geological data, the Permian igneous rocks in the study area are divided into three categories by lithology: dacite, basalt, and pyroclastic rock. Sensitivity analysis shows that the natural gamma curve is sensitive to igneous rocks, and wave impedance is an important parameter to distinguish igneous rocks. Therefore, these two curves are selected as the sensitive curves of igneous rocks in the study area, and the logging responses of different lithologies are analyzed as shown in Table 1. The lithologic curves in the FY area can be calculated using Table 1, which lays the foundation for geostatistical parameter analysis and inversion.

Table 1. **Lithologic logging response characteristics of igneous rocks in the FY area of the northern Tarim Basin**

Igneous lithology	Natural gamma value (GAPI)	P-impedance value ($kg/m^3 \cdot m/s$)
Dacite	100–190	>1.17e + 07
Basalt	30–60	>1.17e + 07
Pyroclastic rocks	50–190	6e + 06~1.17e + 07

Constrained sparse-spike inversion

Constrained sparse-spike inversion (CSSI) is a recursive inversion method based on the convolution model, which takes seismic data into account and transforms the seismic reflection information into wave impedance information, so that the rule of spatial distribution of the physical parameters of the formation is obtained (Xu et al., 2010; Yang et al., 2011). The CSSI method that identifies the igneous lithology and establishes the igneous velocity model can help to rapidly obtain lithologic information on the Permian igneous rocks in the FY area, and it can reflect the spatial distribution of physical parameters of igneous rocks on the whole.

Figure 1 shows the results of inversion of the Permian igneous rocks in the FY area, which elementarily reflects the law of development of igneous rocks in the longitudinal direction. The igneous-rock lithology in the

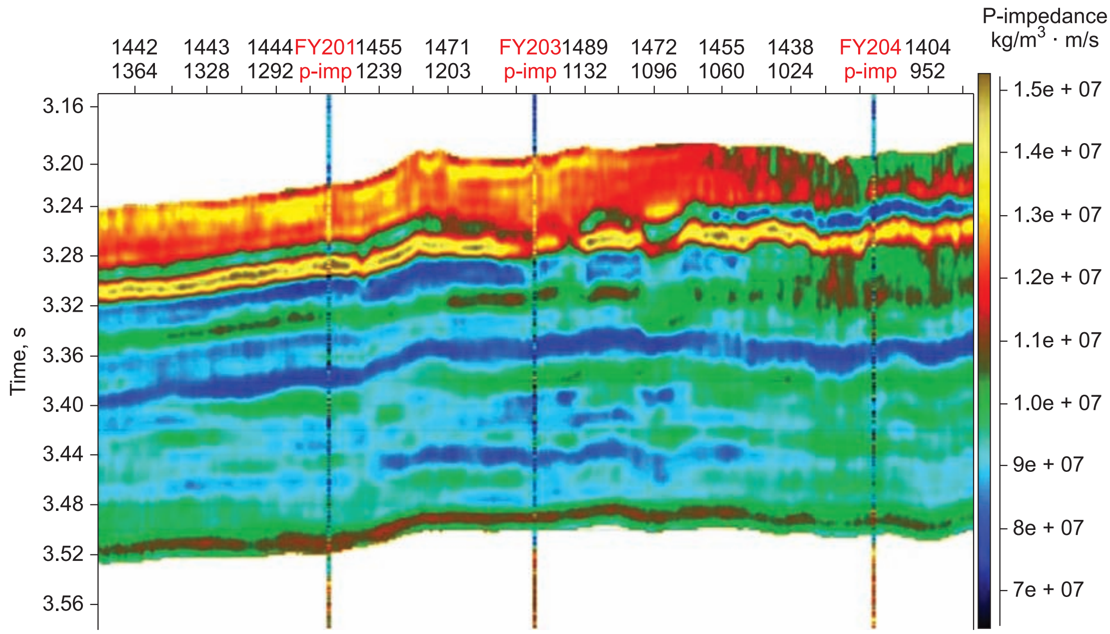

Fig. 1. Constrained sparse-spike inversion section of the FY201, FY203, and FY204 wells.

upper Permian is dominated by dacite and basalt, both with a high impedance value, and the underlying igneous rocks are pyroclastic rocks with a low wave impedance value. The inversion result is consistent with the law of geologic recognition, and there is a relatively continuous pyroclastic interlayer between dacite and basalt, which updates the law of distribution of Permian igneous rocks in the FY area. However, owing to the limitation of vertical resolution, more details cannot be reflected, and geologic inversion is utilized to further improve the vertical resolution of the inversion results. CSSI is an important part of geostatistical inversion. Well seismic calibration, time–depth transformation, fine geologic model establishment, and seismic wavelet extraction will be used into geostatistical inversion, and the absolute impedance of the deterministic inversion is used to obtain the horizontal variation function.

Optimization of geostatistical parameters

The geostatistical parameters mainly include the probability density function (PDF) and variation function. The probability density function describes the possibility of a distribution of elastic parameters corresponding to a particular rock facies. The types of the probability density function include the Gauss-type function, equal distribution function, uniform distribution function, and logarithmic Gauss-type function. The data show that the Gauss function can reflect the distribution of data sample points better, as shown in Fig. 2. Therefore, the Gauss function is used to analyze the logging impedance data on igneous rocks of different lithologies in the FY research area. Figure 2 shows the wave impedance frequency distribution histogram and the Gaussian transformation curve of the pyroclastic rocks in the TT2 layer with an average value of 9.24×10^6 and a standard deviation of 8.62×10^5.

The variation function describes the transverse and longitudinal structure and scale of the geologic features, which means the size of different lithofacies and its attributes in the spatial distribution pattern and the change scale. It is used to describe the spatial correlation of different lithofacies data. The variation function is defined as:

$$r(h) = \frac{1}{2N(h)} \sum_{i=1}^{N(h)} [z(u_i) - z(u_i + h)]^2 , \tag{3}$$

where h is the lag distance, and r is the variation function value; $N(h)$ is the number of distance h, and $z(u_i)$ is a regional variable.

The variable range is an important parameter of the variation function, representing the maximum correlation distance in space (Goovaerts, 1994; Guo et al., 2015; Zhang et al., 2017). The larger the range, the larger the correlation scale indicating the spatial distribution of the regional variables, the slower and the less random the change rate. Since the logging data have a high longitudinal resolution, the sample of logging data is used to calculate the vertical variation function, and the horizontal variation function is calculated from the seismic inversion body with higher lateral resolution. The scientific and accurate variation function can make the geostatistical inversion accurately reflect the spatial distribution characteristics of igneous rocks in the FY area. Figure 3 shows the vertical variation function curve of the wave impedance of pyroclastic rocks of the Permian TT2 layer in the FY area. It can be seen that the variable range is small, which indicates that the pyroclastic rocks are thin and their lithology changes rapidly.

Signal-to-noise ratio and quality control

After analysis of the probability density function and variation function, the random simulation and geostatistical inversion can be carried out. However, in the inversion, it is necessary to determine the weight of the seismic data, that is, the signal-to-noise ratio (SNR), the range of which should be between 1 and 30 dB. The higher the SNR, the smaller the residual. Figure 4 shows the SNR histogram of the CSSI results of the Permian igneous rock in the FY area. Most of the SNR are centered between 10 and 25 dB, which also reflects that the CSSI results of the Permian igneous rock in the FY area match well with the true

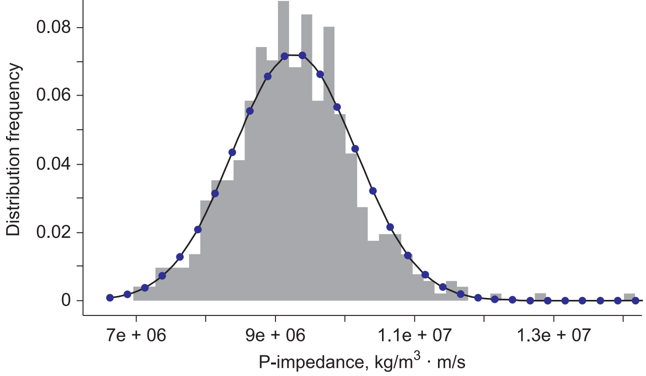

Fig. 2. P-impedance Gaussian transformation of pyroclastic rocks of the TT2 layer in the FY work area.

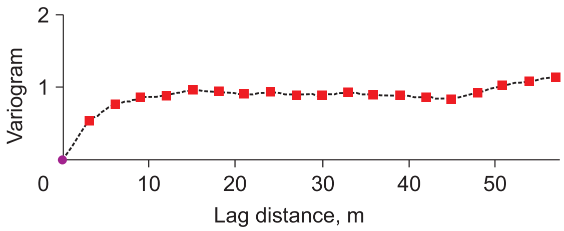

Fig. 3. P-impedance vertical variation function of pyroclastic rocks of the TT2 layer in the FY work area.

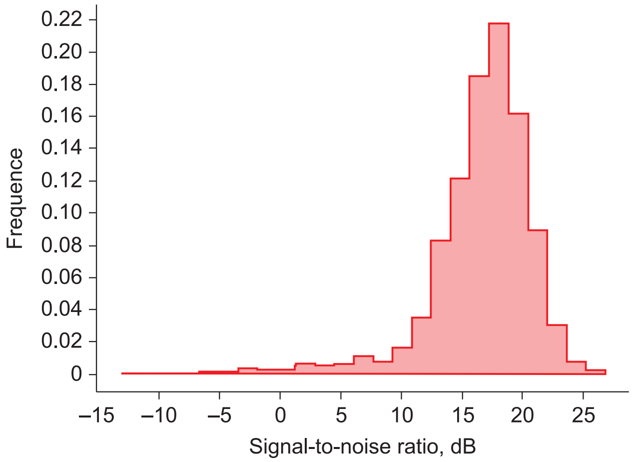

Fig. 4. SNR histogram of the CSSI results for the Permian igneous rocks in the FY area.

seismic record. After several tests, the SNR was determined to be 18 dB.

In the process of geostatistical simulation and inversion, quality control is required to check the correctness of the inversion results (Dong et al., 2013). In the process of geostatistical simulation, the quality control content is mainly to observe the simulated profile and the CSSI profile. The distribution, scale, lithology ratio, and connectivity of the rock obtained by the two methods should be basically identical without overemphasizing the details in the process of geostatistical inversion, in addition to comparing the consistency between the geostatistical inversion profile and the CSSI profile. There is also a test method, the well extracting test, which can be performed in two ways to check the result of inversion. One is to observe whether the inversion body around the well is consistent with the well lithologic curve in the inversion profile. The other is to compare the extracted geostatistical inversion wave impedance curve of the well point with the original wave impedance curve of the well.

CASE STUDY

General geology and characteristics of igneous rocks of the work area

The FY study area is located on the southwestern slope of the Lunnan low uplift, North Tarim uplift. The area is near the Luntai uplift in the north, the Northern depression in the south, the Yingmaili low uplift in the west, and the Lunnan low uplift in the east. The total area of the full fold of the FY region is 588.2 km^2. Drilling revealed thick igneous rock with a thickness of 500–700 m and abruptly varying lithology and velocity in both the lateral and vertical directions. There are ten wells in the FY area, and all of them are drilled into thick igneous rocks. According to the types of rock structure, the rocks are divided into two major categories: volcanic lava and pyroclastic rocks. Volcanic lava is dominated by dacite and basalt, while pyroclastic rocks are dominated by tuff and tuffaceous sandstone and mudstone. According to the chemical type and mineral composition, the igneous rocks are divided into three categories: basic, intermediate, and acidic, but the distribution of intermediate andesite is limited. The basic basalt and acidic dacite are mainly dominant. Figure 5 is a synthesis column map of the FY201 wells in the FY area. In the figure, the GR and acoustic logging responses corresponding to typical seismic sections and cuttings microsection of different igneous rocks are displayed.

The two logging curves in the igneous rock segment are more stable after entering the Permian, and they have a sudden change in the lower igneous rock segment. It shows that the acoustic logging curve is changed from low to high and then low, and the natural gamma value is changed from high to low. Then the two curves remain stable, and the mutation occurs again in the pyroclastic rocks segment. According to the responses, the Permian in the FY area can be divided into three sections: upper, middle, and lower. In the upper section, the GR values are high, and the lithology is dominated by acidic rocks. In the middle section, the GR values are low, about 30–50 API, and the lithology is dominated by basic rocks. The logging curves of the lower section vary greatly, while the lithology of igneous rocks varies greatly. By taking cuttings and identifying a cuttings microsection under a microscope, it is found that the crystal fragments of acidic dacite at 4550 m are plagioclase, quartz, and oxidized amphibole. The basic basalt is found at 4610 m with an intersertal and implicit structure. The matrix is microcrystalline plagioclase, pyroxene, magnetite, and crystalline. In addition, there is tuffaceous fine sandstone with calcite found in the crumbs at 4750 m.

Integrating logging and seismic data and analysis of the cuttings microsection, we obtained the general lithology distribution pattern of Permian igneous rocks in the FY area. The lithology of igneous rocks in the upper Permian is dominated by dacite, and the middle part is dominated by basalt, while the lower part is composed of pyroclastic rocks dominated by tuff and tuffaceous sandstone and mudstone. However, the thickness of igneous rocks with complex lithology in the FY area is large. If there are other lithologies in each igneous rock segment, fine lithologic inversion is needed to identify them.

Analysis of the effect of geostatistical lithologic inversion

Through the geostatistical inversion of the Permian igneous rocks in the FY study area, ten types of igneous probabilities are obtained by ten sorts of realizations, owing to the large work area and the large amount of calculation. Figure 6 shows the geostatistical inversion section of the FY201, FY203, and FY204 wells. Compared with Fig. 1, the rock shape and the scale of distribution of the two wave impedance profiles are roughly the same. Moreover, the wave impedance around the wells in the geologic inversion section of igneous rocks

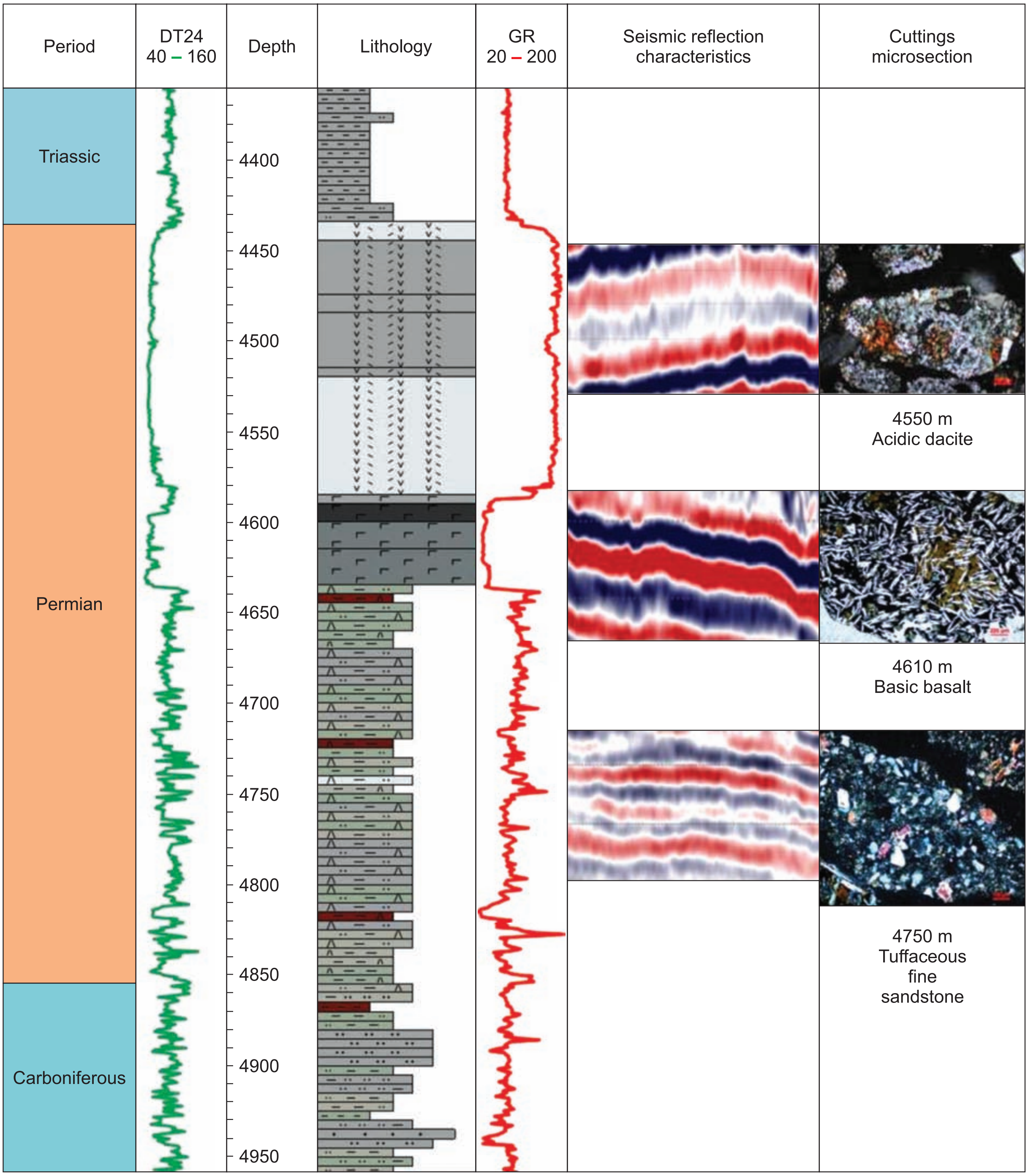

Fig. 5. Comprehensive strata log diagram of the FY201 well.

matches with the well logging data obtained by wave impedance. This verifies that the geostatistical inversion can correctly reflect the lithologic and physical distribution characteristics of igneous rocks of the FY area.

In the lithologic resolution, the constrained sparse-spike inversion in Fig. 1 roughly depicts the changes in lithology, and details are not rich enough. In Fig. 6, some of the thin layers of low-velocity lithologic bodies are identified in the upper part of the Permian, and in the pyroclastic rocks formation, the lower part of the Permian, several sets of high-velocity igneous rocks are identified. The longitudinal resolution is greatly improved.

The FY1 wells revealed two sets of basic basalts, which are easy to distinguish, owing to their lower natural gamma value between 30 and 50 GAPI. The continuity of the phase axis is good. Figure 7 is the identification of the cross section of the FY1 well of basalt to compare the detail recognition ability of constrained sparse-pulse inversion and geostatistical inversion. The basalt contour identified by geostatistical inversion is clearer and more natural. In summary, the geostatistical inversion identifies the igneous rocks with high accuracy and resolution, and the effect is good.

Lithologic distribution analysis of Permian igneous rocks in the FY area

Ten kinds of igneous rock lithology probabilities were acquired by geostatistical inversion, and the probability bodies of the three lithologies were obtained: a dacite probability body, a basalt probability body, and a pyroclastic rock probability body. Figure 8 shows the three lithologies probability profiles of the FY201, FY203, FY204, and FY202 wells, and the color in the profiles is the probability value of a certain lithology. From Fig. 8*a*, it can be known that the dacites are mainly located in the upper part of the Permian, where several sets of relatively continuous “other lithologic bodies” are also located. At the same time, the probability of the dacite in the lower part of the Permian is below 10%. Figure 8*b*, shows the basalt probability profile. The temperature of the basaltic magma is high, usually above 1100 °C. The viscosity is low, and the bursting ability is weak. Therefore, based on the seismic and geological data, the relatively continuous high-probability strata in the upper parts of Fig. 8*b*, can be predicted as basalt. In contrast, the upper and lower intermittent high-probability rock bodies are considered false information, not basalt. It can be seen from Fig. 8*c*, that the stratum lithology under the basalt in the Permian is dominated by pyroclastic rocks, and there are three to four sets of pyroclastic rocks in the upper Permian. It can be concluded that the “other lithologic body” in Fig. 8*a*, is composed of pyroclastic rocks.

Comprehensive Figs. 6 and 8 and the lithologic distribution in the general geology, the lithologic distribution pattern of igneous rocks in the Halahatang FY area in the Permian can be further updated. The main lithology of the upper Permian is dacite, of which there are three to four sets of pyroclastic rocks. There is a relatively continuous pyroclastic rocks interlayer between dacite and basalt, and the stratum lithology under the basalt is dominated by pyroclastic rocks.

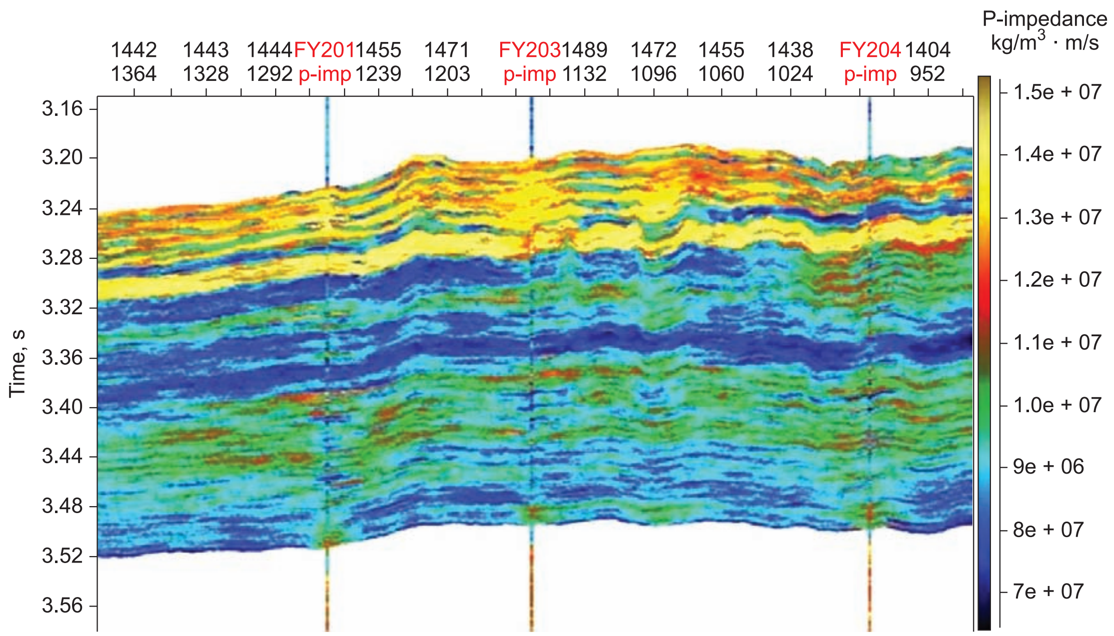

Fig. 6. The geostatistical inversion section of the FY201, FY203, and FY204 wells.

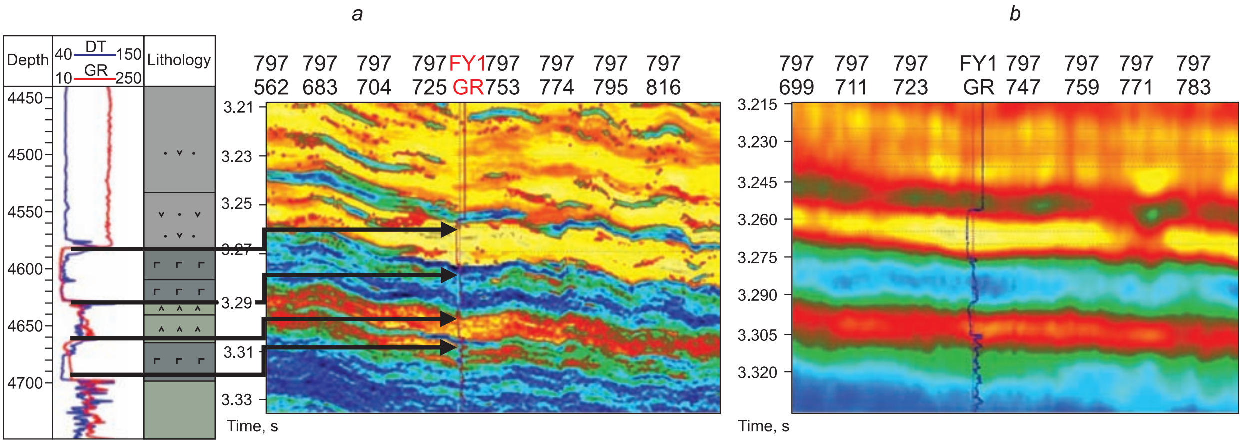

Fig. 7. Comparative analysis of inversion section of the FY1 well. ***a*****, Geostatistical inversion;** ***b*****, constrained sparse-pulse inversion.**

Analysis of the effect of velocity modeling in geostatistical inversion

The high-resolution igneous-rock impedance obtained by geostatistical inversion is transformed into igneous-rock velocity using the empirical transformation formula, which is obtained by fitting the velocity and density data in the region. It can better reflect the characteristics of the igneous rocks. After the transformation, the lithology resolution of igneous rocks is kept unchanged. Thus, the high-precision velocity model of the Permian igneous rocks, based on geostatistical inversion in the FY area, is obtained. To reflect the accuracy of the velocity model and the ability to distinguish the igneous rock, the pseudo-velocity curves of the FY201, FY203, and FY204 wells are extracted. At the same time, we extract the pseudo-velocity curve of the CSSI velocity and compare it with the original velocity curve to analyze the effect of velocity modeling. The comparison of the three velocity curves is shown in Fig. 9. The cyan curve is the original velocity obtained by the well logging; the blue curve is the pseudo-well velocity extracted by the CSSI velocity model; the red curve is the pseudo-well velocity extracted by the high-precision velocity body obtained by the geostatistical inversion.

It can be seen from Fig. 9 that the velocity curve obtained by CSSI is relatively smooth and can reflect the velocity trend in the longitudinal direction of the igneous rocks, but the velocity detail information is not enough. The velocity curve obtained by geostatistical inversion is in good agreement with the original velocity curve of the wells and has high lithological resolution ability. The details of the velocity variation are also rich, which can reflect the velocity information on the underground strata more realistically.

To quantitatively analyze the precision of inversion velocity, the CSSI velocity and geostatistical inversion velocity of YM4, FY102, FY104, FY201, FY203, FY204, and other well points are extracted, and the YM4 well is the verification well, which is not involved in the inversion. The average velocity of the Permian in each well is obtained and compared with the original average velocity of each well. Then the velocity error under two inversion methods is calculated (Table 2). The velocity model obtained by the geostatistical inversion is maintained at a good lithologic resolution, and the velocity accuracy is high. The error is controlled within 2%. Therefore, compared with the commonly used velocity modeling method, geostatistical inversion velocity modeling has a high precision and a superior lithologic resolution.

After comparing the numerical accuracy, the high-precision igneous-rock velocity model based on geostatistical inversion and the conventional strata-bound velocity model are applied to the seismic data process-

Table 2. **Comparison of velocity errors between two inversion methods**

Inversion velocity analysis		YM4	FY102	FY104	FY201	FY203	FY204	Mean
Original velocity from well	Value, m/s	4368.6	4376.3	4359.7	4359.7	4319.9	4305.4	4348.3
Velocity from CSSI	Value, m/s	4342.7	4370.9	4304.2	4304.1	4314.6	4283.4	4319.9
	Error	–0.59%	–0.12%	–1.27%	1.04%	–0.12%	–0.51%	–0.26%
Velocity from geostatistical inversion	Value, m/s	4401.6	4386.2	4285.3	4344.1	4342.6	4290.1	4341.7
	Error	0.75%	0.23%	–1.71%	1.98%	0.53%	–0.36%	0.23%

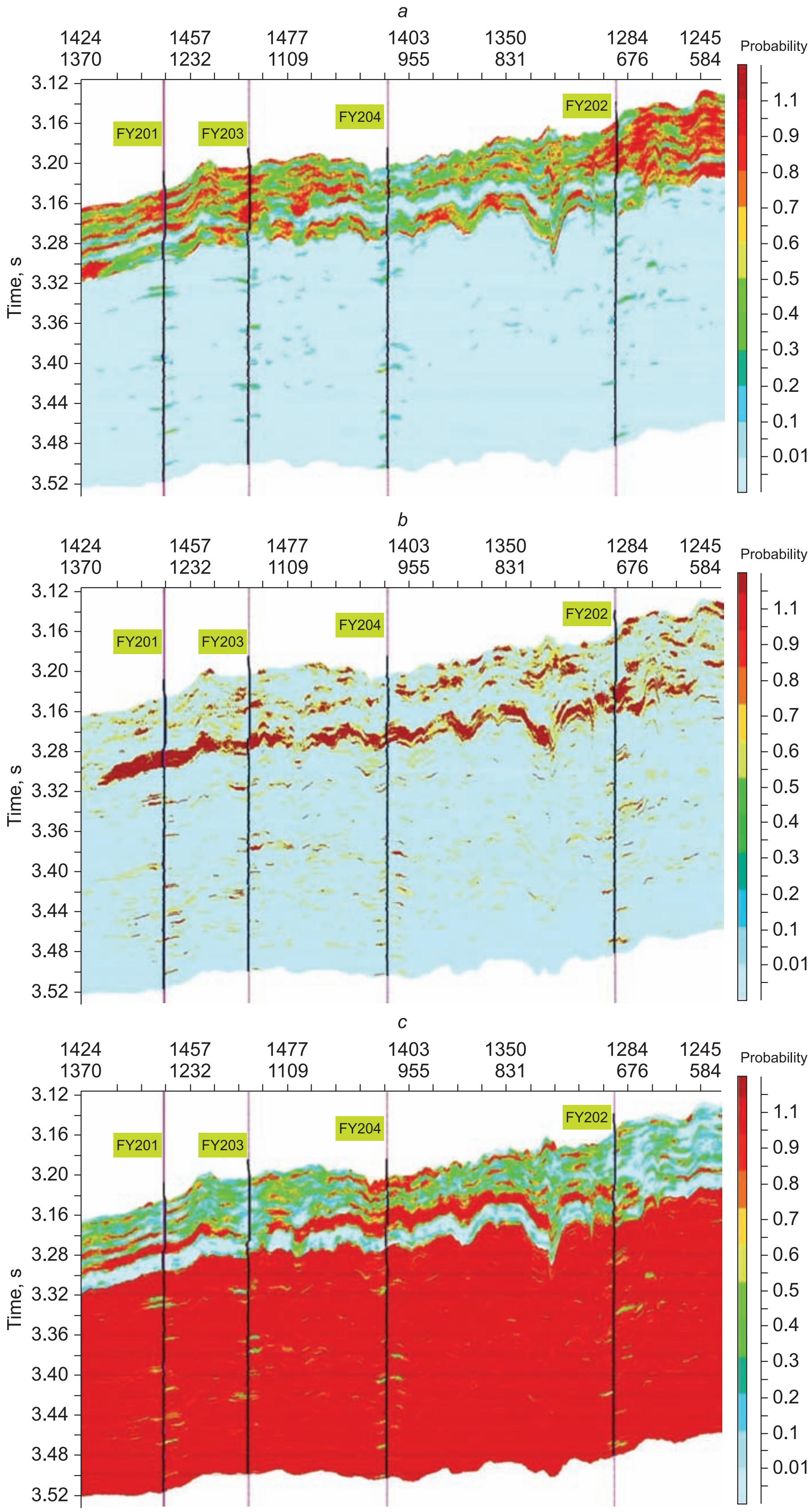

Fig. 8. The three lithologies probability profiles of the FY201, FY203, FY204, and FY202 wells. ***a*****, Dacite probability body;** ***b*****, basalt probability body;** ***c*****, pyroclastic-rock probability body.**

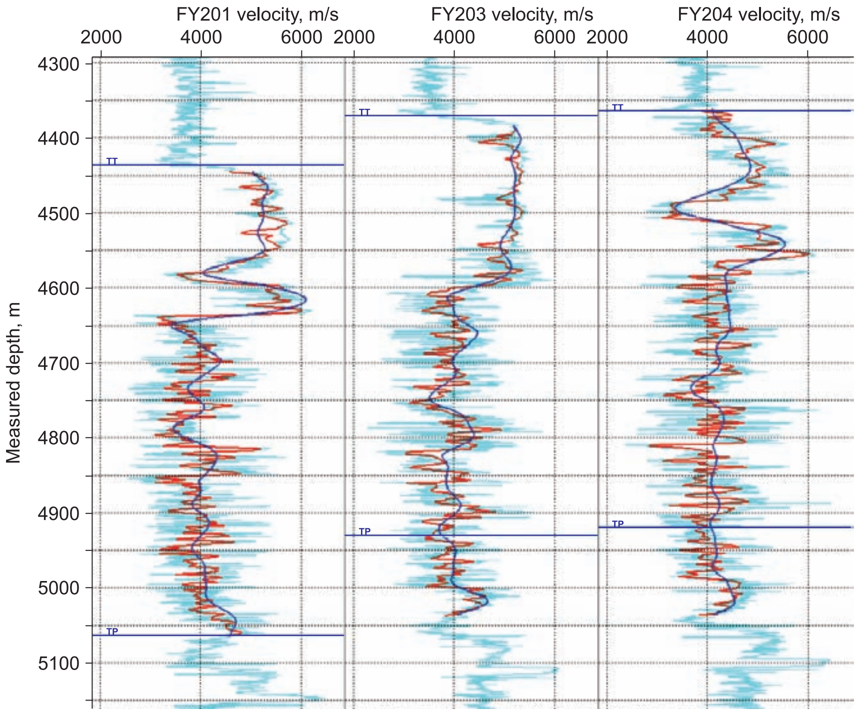

Fig. 9. Comparison of pseudo-velocity curves of different inversion methods in the FY201, FY203, and FY204 wells.

ing. Figure 10 shows the comparison of the migration results. Figure 10*a*, shows the offset profile obtained using the conventional strata-bound velocity model to process the seismic data, and Fig. 10*b*, shows the offset profile obtained using the high-precision velocity model in this study. If we compare the two profiles, the internal description of igneous rocks is clearer in the profile of Fig. 10*b*. The signal-to-noise ratio is improved, and the continuity is enhanced. Therefore, in addition to reservoir prediction, geostatistical inversion can be used as an effective method to establish the fine velocity model of igneous-rock or other lithology and can provide a high-precision velocity model for seismic data processing.

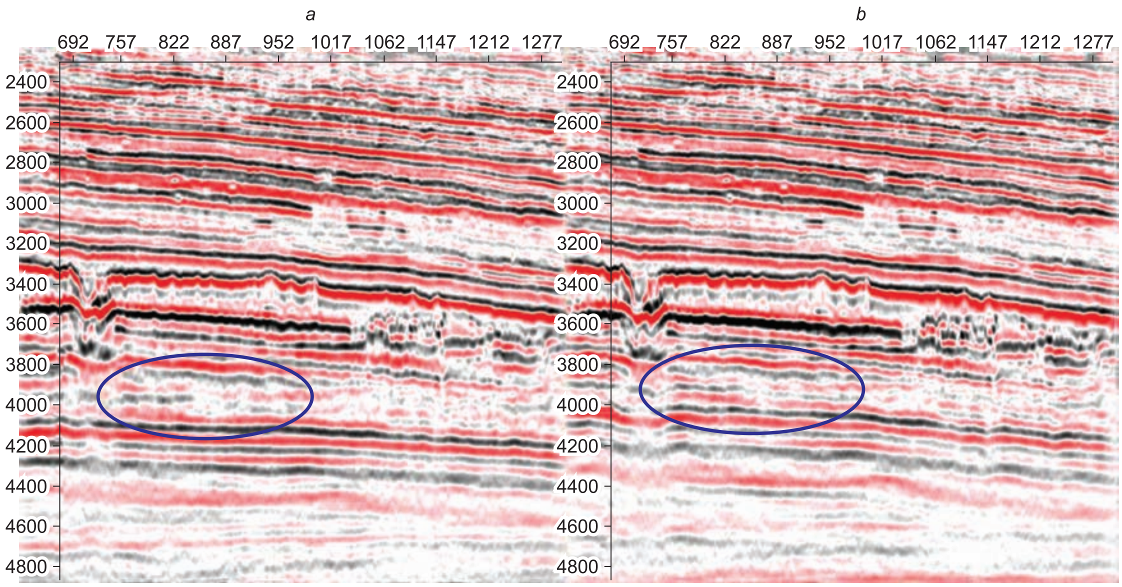

Fig. 10. Comparison of offset imaging using different velocity models. *a*, The conventional strata-bound velocity model; *b*, geostatistical inversion velocity model.

CONCLUSIONS

In this study, a geostatistical inversion method is applied to lithology identification and velocity modeling of the Permian thick igneous rock in the FY area of the northern Tarim Basin. The following conclusions are made:

CSSI takes into account seismic data and can roughly reflect the distribution characteristics of lithology. On this basis, the geostatistical inversion is used to identify the igneous-rock lithology, which depicts the shape and contour of the igneous rocks more clearly. By analyzing the wave impedance and the probability body of different igneous-rock lithologies, a more accurate distribution pattern of Permian igneous rocks in the FY area is obtained. That is, the lithology of igneous rocks in the upper Permian is dominated by dacite, of which there are three to four sets of pyroclastic rocks. The main igneous rock in the middle Permian is basalt. The igneous rocks in the lower Permian are pyroclastic rocks with complex lithology which is dominated by tuff and tuffaceous sandstone and mudstone. In addition, there is a relatively continuous pyroclastic rock interlayer between dacite and basalt;

The velocity model obtained by geostatistical inversion can reflect the details of the velocity variation of the Permian igneous rock. The drilling results have verified the high accuracy of the geostatistical inversion velocity modeling. The velocity error of the well point is controlled within 2%, and the average error is 0.23%. It can provide a high-precision igneous-rock velocity model for formation pressure prediction and seismic data processing. It also provides a reliable basis for variable velocity mapping and trap ascertainment and ultimately guides the work of oil exploration and development;

Lithological information obtained by geostatistical inversion is rich, and the resolution is high. However, the calculation of inversion is large, and the statistical work is more complex. In addition, the inversion work is more suitable for areas that have more drilling wells. In contrast, other modeling methods, such as CSSI and tomographic inversion, are more suitable for large-scale and fast-velocity modeling.

This work was supported by the project funded by the Priority Academic Program Development of Jiangsu Higher Education Institutions, the China Postdoctoral Science Foundation (grants No. 2014M551703 and 2018M630631), and the Fundamental Research Funds for the Central Universities (grants No. 2012QNA62 and Isujbky-2019-54).

REFERENCES

Bellatreche, K.-E., Couch, A., Evans, R., 2017. Detailed seismic lithofluid distribution using Bayesian stochastic inversion for a thinly bedded reservoir: A case study over Huntington UK Central North Sea. Interpretation 5 (3), SL25–SL32.

Cui, Y., Xu, Y., Peng, G., 2016. Igneous rock identification and velocity modeling based on several seismic inversion methods in Halahatang area. J. Northeast Pet. Univ. 40 (4), 54–62.

Dong, Q., Lu, S., Zhang, X., Shang, J., 2013. Selection of parameters and reliability analysis of results in geostatistical inversion method. Geophys. Geochem. Explor. 37 (2), 328–332.

Goovaerts, P., 1994. Comparative performance of indicator algorithms for modeling conditional probability distribution functions. Math. Geol. 26 (3), 389–411.

Guo, Z., Sun, L., Jia, A., Lu, T., 2015. 3-D geological modeling for tight sand gas reservoir of braided river facies. Pet. Explor. Dev. 42 (1), 83–91.

Luo, F., 2006. Study on Characteristic and Predicting Technology of Igneous Rocks in Tazhong Area of Tarim Basin. China Univ. Geosci., Beijing.

Naviset, S., Morley, C.K., Naghadeh, D.H., Ghosh, J., 2017. Sill emplacement during rifting and inversion from three-dimensional seismic and well data, Phitsanulok Basin, Thailand. Geosphere 13 (6), 2017–2040.

Pereira, Â., Nunes, R., Azevedo, L., Guerreiro, L., Soares, A., 2017. Geostatistical seismic inversion for frontier exploration. Interpretation 5 (4), T477–T485.

Sabeti, H., Moradzadeh, A., Ardejani, F.D., Azevedo, L., Soares, A., Pereira, P., Nunes, R.F.M., 2017. Geostatistical seismic inversion for non-stationary patterns using direct sequential simulation and co-simulation. Geophys. Prospect. 65 (S1), 25–48.

Sammarco, C., Cornwell, D.G., Rawlinson, N., 2017. Ambient noise tomography reveals basalt and sub-basalt velocity structure beneath the Faroe Islands, North Atlantic. Tectonophysics 721, 1–11.

Shen, H., Qin, D., Hou, D., 2016. Predication of super thin reservoir based on geostatistical inversion. SEG Technical Program Expanded Abstracts 2016. Society of Exploration Geophysicists, pp. 2891–2895.

Tamaki, M., Suzuki, K., Fujii, T., Sato, A., 2016. Prediction and validation of gas hydrate saturation distribution in the eastern Nankai Trough, Japan: Geostatistical approach integrating well-log and 3D seismic data. Interpretation 4 (1), SA83–SA94.

Wang, Y., Wang, L., 2013. Application of geostatistical inversion to reservoir prediction in the Western Slope of the northern Xingshugang oil field. Prog. Geophys. 28 (5), 2554–2560.

Xie, H., Xu, Y., Zheng, D., Gao, H., Li, G., Ye, M., Wang, S., 2015. Multi-attribute probabilistic neural network inversion applicated in identifying igneous rocks in RWP area based on cross-validation. China Min. Mag. (2), 154–158.

Xu, Y., Chen, T., Chen, S., Huang, W., Wu, G., 2010. Comparison between several seismic inversion methods and their application in mountainous coal fields of western China. Min. Sci. Technol. (China) 20 (4), 585–590.

Yang, H., Xu, Y., Huang, Z., Chen, S., Yang, Z., Wu, G., Xiao, Z., 2011. Comparison between several multi-parameter seismic inversion methods in identifying plutonic igneous rocks. Min. Sci. Technol. (China) 21 (3), 325–331.

Yu, Z., He, J., 2013. A high resolution method for fluid prediction based on geostatistical inversion. Int. J. Geophys. Accessed 23 November 2020.

Zhang, J., Liu, L., Wang, R., 2017. Geostatistical three-dimensional modeling of a tight gas reservoir: A case study of block S6 of the Sulige gas field, Ordos Basin, China. Energies 10 (9), 1439.

Zhang, S., Liu, T., Gu, H., 2003. Identification of igneous rocks by artificial neural network. Oil Geophys. Prospect. 38, 84–87.

Zhang, Z., Cao, D., Yin, X., Liu, B., Sun, C., 2016. Research and application status of well seismic joint velocity modeling in time-depth conversion. Prog. Geophys. 31 (5), 2276–2284.

Поступила в редакцию 23 ноября 2018 г.,
принята в печать 10 октября 2019 г.